

A numerical analysis of multicellular environment for modeling tissue electroporation

M. Essone Mezeme,¹ G. Pucihar,² M. Pavlin,² C. Brosseau,^{1,a)} and D. Miklavčič²

¹Université Européenne de Bretagne, Université de Brest, Lab-STICC, CS 93837, 6 Avenue Le Gorgeu, 29238 Brest Cedex 3, France

²University of Ljubljana, Faculty of Electrical Engineering, Trzaska 25, 1000 Ljubljana, Slovenia

(Received 26 January 2012; accepted 15 March 2012; published online 3 April 2012)

Simulations probing the conductivity changes of three-dimensional models of biological tissues consisting of random ternary core-shell sphere packings with different spatial scales are described. We investigate the temporal evolution of the electric conductivity of these packings during application of an electric field with magnitude either below or above the value leading to cell membrane electroporation. The fraction of electroporated cells can be described by a hyperbolic tangent function of the electric field. The collective physical processes causing the transient permeability of the cell membranes can be understood by analogy with the physics of a two-state system with an external field. © 2012 American Institute of Physics. [<http://dx.doi.org/10.1063/1.3700727>]

Electroporation (EP) permits the uptake of poorly permeant molecules, like fluorescent probes, proteins, and DNA fragments, because it transiently increases the permeability of the cell membrane.^{1,2} Since the discovery of EP, the question of the physical mechanisms that temporarily disturb the phospholipid bilayer of the plasma membrane has been a forefront topic in the field of EP. EP results in the significant increase in the electrical conductivity and diffusive permeability of the cell membrane caused by a large pulsed electrical field E ,¹⁻⁵ i.e., typically a few kV cm^{-1} lasting from $1 \mu\text{s}$ to few ms. A number of studies have reported that EP depends on the local induced transmembrane voltage (ITV) induced by the external electric field. It has also been shown that a specific ITV threshold exists for the manifestation of the EP phenomenon (typically from 0.2 V to 1 V, depending on the cell type), i.e., only the cells within areas where $\text{ITV} \geq \text{ITV}_{\text{th}}$ are electroporated. If the field is too strong or lasts too long a time, the viability of the cells is compromised and EP is said to be irreversible.

However, there has arguably been a lack of theoretical models capable of explaining the diversity of findings concerning the EP of biological materials, e.g., tissue.⁵ In particular, the main focus of experimental studies has been on dense suspensions of cells and tissues.⁵ A tissue is an ensemble of cells that together carry out a specific function, e.g., in a connective tissue (Fig. 1(a)) cells of diameter between 10 and $20 \mu\text{m}$ are spread through an extracellular fluid. Reconstructing the three-dimensional morphology of biological objects such as tissues using first-principles computations is a formidable challenge (see, e.g., Ref. 6 for a recent review and references). Numerical modeling studies probing the statistical structure and the electric response of these complex and heterogeneous environments have been limited. This question has been studied by considering, e.g., the mesh transport network method, which utilizes equivalent circuit networks to simulate nonlinear, coupled transport phenomena,⁷ finite difference method,⁴ molecular dynamics,⁸ or finite element (FE) simulations.^{3,9}

Early studies²⁻⁴ showed that EP of cell membranes arises in specific regions (“hot spots”). It remains unclear, however, how close proximity of cells in tissues affects the formation of hot spots. What remains of crucial importance is whether it is possible to evaluate the fraction of electroporated cells of an assembly of cells modelling a tissue. It was indicated in Ref. 5 that the use of fluorescent dyes allowed experiments to reveal the collective behavior associated with the cell membrane EP of dense cell suspensions. As the cell density increases, the fraction of electroporated cells is found to decrease.⁵ The density increase favors electric shielding of cells, which, in turn, leads to a decrease of the ITV.⁵ It has also been recognized for some time that the electric-field induced stretching of the membrane exhibits a peculiar anisotropy. For spherical cells, it is well known that anisotropy should manifest itself as a $\cos \theta$ dependence for the electric

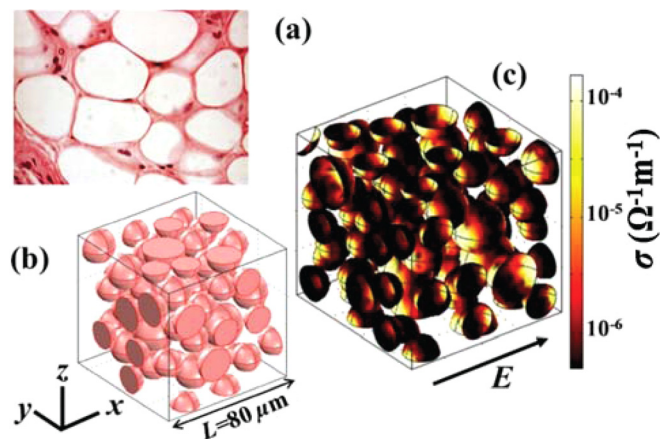


FIG. 1. (a) Loose connective tissue composed of adipose cells. The source of image from Huclova *et al.*, J. Phys. D 43, 365405 (2010). Copyright 2010, IOP. (b) A specific realization of our multicellular tissue model consisting of randomly positioned spherical CS structures with three cell sizes: 8, 10, and $12 \mu\text{m}$. (c) Spatial patterns of the local increase in membrane electric conductivity illustrating the spatial distribution of hot spots in randomly positioned CS structures. The cell density is set to 28 vol. %. The electric conductivity is computed $4 \mu\text{s}$ after the onset of the field with magnitude of $1 \text{ kV cm}^{-1} > E_{\text{th}} = 0.45 \text{ kV cm}^{-1}$. The color bar on the right gives the values of the membrane conductivity.

^{a)}Electronic mail: brosseau@univ-brest.fr.

field components^{1,2} and as a $\cos^2\theta$ for the Maxwell stress tensor components² at membrane interfaces, where θ denotes the angle from the axis formed by the line passing through its origin and parallel to the applied electric field. Conceptually, the local and anisotropic characters of cells' EP pose fundamental problems in understanding both the numerical simulations and observations of tissues.

One of the main purposes of this letter is to argue that by using a parsimonious, computationally simple stochastic three-dimensional model of packings of spheres of three sizes (ternary sphere packings), one can obtain, by computing the changes in electric conductivity due to EP, results which are consistent with the above mentioned observations. Achieving an accurate quantitative description of the fraction of electroporated cells p of a tissue subjected to a transient electric field is a daunting task. Here, we use this multiscale model to predict p by monitoring the membrane electric conductivity as a function of the exogenous electric field magnitude. This prediction is shown to agree well with experimental observations.¹⁰

The core-shell (CS) model of biological cells has been recognized as a fertile ground in respect of their dielectric relaxation mechanisms.¹¹ An important aspect of this continuum model is that the potential drop over the cell size occurs almost entirely across the membrane since there is a high conductivity contrast between the insulating membrane (nanosized shell) and the conducting cytoplasmic core. We model a tissue with a random assembly of CS spherical structures with three cell radii 8, 10, and 12 μm . These values are consistent with the cell size distribution observed in reflectance in biological tissues (see Fig. 1(a)).¹² Even if real tissues, however, are not composed of rigid and immobilized cells, we will restrict our study to undeformable sphere-shaped cells. The algorithmic method consists of placing the CS spherical particles in a random manner without any overlap between them employing an internal MATLAB function, which uses a lagged Fibonacci random numbers generator. The general recipe can be used to construct various models, depending on the cell radius and number assignments. An example of such geometric model is shown in Fig. 1(b) along with the corresponding local distribution in membrane electric conductivity (Fig. 1(c)). We shall use the asymptotic DeBruin-Krassowska (DBK) model of EP for a single cell based on the Smoluchowski equation. The full description of DBK model is given in Refs. 4 and 13. Representative values for the primary parameters defining the assembly of CS structures and the cell and tissue EP are identical to those of Table I in Ref. 3. The FE method presented here solves Laplace's equation in time domain to obtain the distribution of the electric potential in the model. The effective conductivity of the cell suspension σ is obtained from the linear response of the current density $j = \sigma E$ induced by the exogenous electric field. The time rise is 0.1 μs . It was implemented within COMSOL using a Heaviside function. The first-principle calculations were performed in COMSOL MULTIPHYSICS, a commercial program that uses FE methods to solve partial differential equations.^{14,15} The simulations use an $80 \times 80 \times 80 \mu\text{m}^3$ computational domain with electrically insulated boundary conditions for the y - z and x - z planes (conservation of the electric current density), adopting previ-

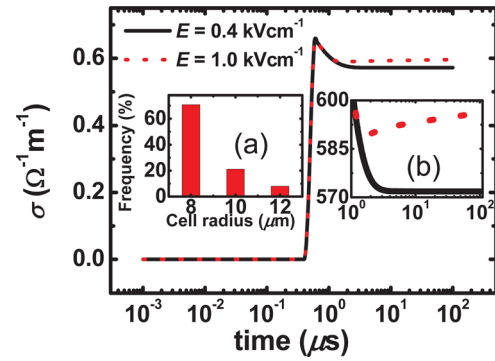


FIG. 2. Time dependence of the average electric conductivity σ calculated for 15 realizations of the tissue model shown in Fig. 1(b). The solid line (black) is $\sigma(t)$ for $E = 0.4 \text{ kV cm}^{-1} < E_{\text{th}} = 0.45 \text{ kV cm}^{-1}$ and the dotted line (red) is $\sigma(t)$ for $E = 1 \text{ kV cm}^{-1} > E_{\text{th}} = 0.45 \text{ kV cm}^{-1}$. The cell density is set to 28 vol. %. (a) Size histogram for three cell radii used in the tissue model. (b) Inset showing an enlarged view of the main frame between 1 and 100 μs .

ously published techniques.^{4,5} Tetrahedral meshes were used in these calculations. The number of tetrahedral elements varies between 40 000 (20 vol. % of cells) and 55 000 (for the denser configuration of cells.). The membrane was replaced by a thin surface to which a boundary condition is assigned between the cytoplasm and the extracellular medium. That is the mesh elements corresponding to the membrane are avoided.⁵ The average computational time of a typical simulation of the multicellular tissue model shown in Fig. 2 is about 1 h. A uniform external electric field, with magnitude E and rise time t_r , is applied along the x -axis.

The changes in the σ during electric field excitation are shown in the main frame of Fig. 2 for the average of 15 realizations of a random cell model arrangement consisting of CS spheres of three sizes, each realization having a volume fraction set to 28%. The increase of σ vs time produced by $E = 1 \text{ kV cm}^{-1} > E_{\text{th}} = 0.45 \text{ kV cm}^{-1}$ should be interpreted as a plausible evidence of the EP phenomenon.^{16,17} To understand the physical origin of the local σ enhancement exhibited by tissue models, one must understand how local interactions between cells affect the collective charge transport. The primary effect of the field on the cells is the membrane polarization, which creates the ITV. A single spherical cell polarizes with relaxation time constant, which can be written as⁴ $\tau = \frac{R\epsilon\epsilon_0}{h} \left(\frac{1}{\sigma_i} + \frac{1}{\sigma_e} \right)$, where R denotes the cell radius, ϵ the relative permittivity (5) of its membrane of thickness h ($5 \cdot 10^{-9} \text{ m}$), σ_i is the intracellular conductivity ($0.2 \Omega^{-1} \text{ m}^{-1}$), and σ_e is the extracellular conductivity ($1 \Omega^{-1} \text{ m}^{-1}$). For these parameters and for multiple cells situation considered in Fig. 1, the membrane charging time is $\tau \approx 1 \mu\text{s}$ (Fig. 2) and is consistent with a passive resistive-capacitive membrane charging exposed to an electric field. In Fig. 2, once charging is complete ($t > \tau$), the observed increase of σ for $E > 1 \text{ kV/cm}$ corresponds to EP of cells while the curve observed for $E = 0.4 \text{ kV cm}^{-1} < E_{\text{th}}$ is the expected behavior for nonelectroporated cells (Fig. 2(b)). The increase of σ is due to the fact that part of the current, which was flowing around cells, can now flow through the electroporated cells. The collective (macroscopic) tissue response is determined by the local electric field experienced by the individual cells

at the microscopic level. The slight overshoot in $\sigma(t)$ is associated with the capacitive term of the current. The shorter the rise time of the voltage pulse, the higher the overshoot.¹⁶

After having demonstrated that this tissue model provides a satisfactory description of the electrical properties, we now proceed to investigate the influence of cell size polydispersity on σ . Two important observations can be made. First, the larger cells were electroporated first. Second, areas of cell membranes that undergo EP occur in regions where polarization is maximized.

Motivated by the above results, we carried out similar simulations of multiscale tissue model with different densities in order to clarify the relationship between the fraction of electroporated cells p and the applied electric field magnitude E . The fraction of electroporated cells p was calculated for 5 different realizations of the tissue model, with each model having the same cell density, and the values of p were then averaged. Fig. 3 compares the values of $p(E)$ for 3 cell densities ranging from 20 vol. % to 33 vol. % for field duration of 100 μ s. These results lead to the important conclusion that EP initiates at higher E when cell suspension is denser. It is important to note that our calculations are in good agreement with the experimental observations of Ref. 5, where higher cell densities required higher field magnitudes to obtain the same fraction of EP. Physically, dipolar couplings which are effective at the macroscopic scale are important when the polarization is not isotropic. We should underline that from a physical point of view, it is natural to expect a large anisotropic σ in the EP since only a fraction of the cell's area is electroporated during the field exposure (Fig. 1(c)).³ As can be clearly observed in Fig. 3, the sigmoid $p(E) = \left(1 + \tanh\left(\beta(E - E_c)\right)\right)/2$, where β is a constant and E_c is a crossover field, seem to be a universal characteristics for the range of densities investigated in this study. It is worth noting that the curves shown are coherent with the modelling and experimental study of the diffusion-driven transmembrane transport of small molecules caused by electroporation performed by Puc *et al.*¹⁸ Although we came across this finding serendipitously, we would like to question whether this equation explains data better than a simple empirical curve. In fact, this universality can be interpreted in the framework of two-state systems commonly

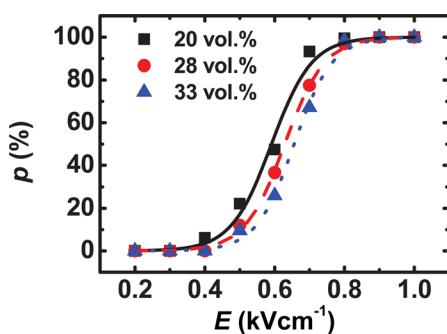


FIG. 3. Fraction of electroporated cells p , as a function of electric field magnitude E for cell densities of (■) 20 vol. %, (●) 28 vol. %, and (▲) 33 vol. %. The results are the averages of 5 random distributions of ternary CS tissue models for a given cell density. The curves are the fits of the hyperbolic tangent law to the calculated data. The field duration is 100 μ s.

encountered in statistical physics, e.g., the archetype models are the spin-1/2 case of paramagnetism and the polarized light,¹⁹ according to which the order parameter follows a hyperbolic tangent law as a function of the exciting field. The above remarks are relevant to our work because the electroporated and non-electroporated cell membranes subjected to the applied electric field can be viewed as the two states in the linear response regime. Taken together, these simulations qualitatively reproduce the features of the hyperbolic tangent law describing the crossover from non-electroporated to electroporated states. Reducing the cell density in the computational domain results in a decrease of E_c (Fig. 3) whereas β is found to be constant and equal to $0.11 \text{ (kV/cm)}^{-1}$.

Cells in tissue are likely to be electroporated at a lower electric field than cells in suspensions. There are still some unresolved issues regarding the role of cell junctions and microstructure present in tissue on cell EP. We expect that a multiscale model with a more realistic representation of tissues will give us valuable insight into the EP phenomenon at the tissue level. For cell densities lower than approximately 10 vol. %, the results would be very similar to those obtained for an isolated spherical cell. However, increasing cell densities would require progressively higher electric fields to obtain the same fraction of electroporated cells (Fig. 3) and this will hold even for cell densities above 33%.

Finally, Fig. 4 compares the values of $p(E)$ obtained from our numerical model for two different field durations. A good agreement between numerical data and the hyperbolic tangent law is found for both curves. The results reveal that the crossover field decreases from 0.7 to 0.63 kV/cm as the duration of the pulse field the application is increased from 4 to 100 μ s with a common value of $\beta \cong 0.11$.

In summary, we have shown that a simple three-dimensional model of tissues that uses random spatial distributions of ternary simple cell models can qualitatively account for predicting the collective electrical response of cells in tissues to applied electric fields. This work provides a convincing example of an *in silico* multiscale model of tissues. Of particular novelty has been the identification of the volume fraction of electroporated cells in the multiscale models of tissue, which can be described with a hyperbolic tangent law. Further numerical experiments for different cell

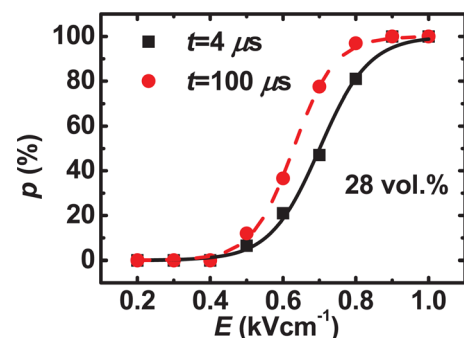


FIG. 4. Fraction of electroporated cells, averaged over 5 disorder realizations, of the tissue model versus applied electric field magnitude for a random distribution of ternary CS cells model with cell density of 28 vol. % for two durations of the electric field E (■) 4 μ s and (●) 100 μ s. Data sets can be fit with the hyperbolic tangent law which is shown as solid line.

size distributions remain to be done to illuminate generalities and/or differences between the present case for which smaller cells are in larger proportion than larger cells. Finally, we observed that our formulation can readily be generalized to spatially distributed CS cell models with irregular shape, e.g., cuboidal epithelial tissue cells, echinocytes.²⁰ The flexibility of multiphysics modeling with FE methods will allow future models to incorporate greater sophistication, simulating also molecular transport across the membranes as well as the electromechanical properties of tissues.²

We acknowledge financial support from the Ph.D. funding programme (Grant programme 211-B2-9/ARED) of the Conseil Régional de Bretagne. This work is also partially supported by Université Européenne de Bretagne through its mobility program. The Lab-STICC is Unité Mixte de Recherche CNRS 6285. This work was in part supported also by Slovenian Research Agency.

¹T. Inoue and R. Krumlauf, *Nat. Neurosci.* **4**, 1156 (2001); D. S. Dimitrov, *Electroporation and Electrofusion of Membranes*, in Handbook of Biological Physics, Vol. 1, edited by R. Lipowsky and E. Sackmann (Elsevier, Amsterdam, 1995), pp. 851-901.

²H. Isambert, *Phys. Rev. Lett.* **80**, 3404 (1998); M. Bier, W. Chen, T. R. Gowrishankar, R. D. Astumian, and R. C. Lee, *Phys. Rev. E* **66**, 062905 (2002); J. C. Weaver and Y. A. Chizmadzhev, *Bioelectrochem. Bioenerg.* **41**, 135 (1996); C. Chen, S. W. Smye, and M. P. Robinson, *Med. Biol. Eng. Comput.* **44**, 5 (2006).

³G. Pucihar, D. Miklavčič, and T. Kotnik, *IEEE Trans. Biomed. Eng.* **56**, 1491 (2009).

⁴K. A. DeBruin and W. Krassowska, *Biophys. J.* **77**, 1213 (1999); K. A. DeBruin and W. Krassowska, *ibid.* **77**, 1225 (1999).

⁵G. Pucihar, T. Kotnik, J. Teissié, and D. Miklavčič, *Eur. Biophys. J.* **36**, 173 (2007); G. Pucihar, T. Kotnik, B. Valič, and D. Miklavčič, *Ann. Biomed. Eng.* **34**, 642 (2006); P. J. Canatella, M. M. Black, D. M. Bonnichsen, C. McKenna, and M. R. Prausnitz, *Biophys. J.* **86**, 3260 (2004); R. Susil, D. Šemrov, and D. Miklavčič, *Electro- Magnetobiol.* **17**, 391 (1998).

⁶B. Magdalena, A. Stolarska, Y. Kim, and H. G. Othmer, *Philos. Trans. R. Soc. London, Ser. A* **367**, 3525 (2009).

⁷K. C. Smith, T. R. Gowrishankar, A. T. Esser, D. A. Stewart, and J. C. Weaver, *IEEE Trans. Plasma Sci.* **34**, 1480 (2006).

⁸A. A. Gurtovenko and I. Vattulainen, *J. Chem. Phys.* **130**, 215107 (2009).

⁹V. Myroshnychenko and C. Brosseau, *Phys. Rev. E* **71**, 016701 (2005).

¹⁰T. Kotnik, G. Pucihar, and D. Miklavčič, *J. Membr. Biol.* **236**, 3 (2010).

¹¹R. Pethig, *Dielectric and Electronic Properties of Biological Materials* (Wiley, New York, 1979); K. R. Foster and H. P. Schwan, *Crit. Rev. Biomed. Eng.* **17**, 25 (1989).

¹²L. T. Perelman, V. Backman, M. Wallace, G. Zonios, R. Manoharan, A. Nusrat, S. Shields, M. Seiler, C. Lima, T. Hamano, I. Itzkan, J. Van Dam, J. M. Crawford, and M. S. Feld, *Phys. Rev. Lett.* **80**, 627 (1998).

¹³W. Krassowska and J. C. Neu, *Biophys. J.* **66**, 1768 (1994); J. C. Neu and W. Krassowska, *Phys. Rev. E* **59**, 3471 (1999).

¹⁴M. E. Mezeme, S. Lasquelles, and C. Brosseau, *Phys. Rev. E* **84**, 026612 (2011); M. E. Mezeme, S. Lasquelles, and C. Brosseau, *Phys. Rev. E* **81**, 057602 (2010).

¹⁵COMSOL MULTIPHYSICS version 3.4, COMSOL MULTIPHYSICS® Modeling Guide, Version 3.5 (Comsol AB, Stockholm, 2008).

¹⁶D. Cukjati, D. Batiuskaite, F. André, D. Miklavčič, and L. M. Mir, *Bioelectrochemistry* **70**, 501 (2007).

¹⁷M. Pavlin, M. Kandušer, M. Reberšek, G. Pucihar, F. X. Hart, R. Magjarić, and D. Miklavčič, *Biophys. J.* **88**, 4378 (2005).

¹⁸M. Puc, T. Kotnik, L. M. Mir, and D. Miklavčič, *Bioelectrochemistry* **60**, 1 (2003).

¹⁹C. Brosseau, *Fundamentals of Polarized Light: A Statistical Approach* (Wiley, New York, 1998).

²⁰S. Huclova, D. Erni, and J. Fröhlich, *J. Phys. D* **43**, 365405 (2010).